Limnol. Oceanogr., 59(3), 2014, 798–810

doi:10.4319/lo.2014.59.3.0798

High rates of daytime respiration in three streams: Use of $\delta^{18}O_{O_2}$ and O_2 to model diel ecosystem metabolism

Erin R. Hotchkiss [a,*] and Robert O. Hall, Jr.

Program in Ecology, Department of Zoology and Physiology, University of Wyoming, Laramie, Wyoming

Abstract

Photosynthesis and respiration determine the carbon and oxygen (O_2) balance of ecosystems. Current methods used to estimate ecosystem respiration (ER) do not include diel ER fluctuations, which limit testing predictions about short-term drivers of ecosystem metabolism. Diel changes in $\delta^{18}O_{O_2}$ can be used to estimate diel ER due to discrimination against $^{18}O_{O_2}$ during respiration. We monitored diel $\delta^{18}O_{O_2}$, O_2, light, and water temperature in three Wyoming streams and measured respiration fractionation (α_R) against $^{18}O_{O_2}$ in dark benthic flow chambers in two streams. The ranges of measured and literature α_R values were used to estimate uncertainty in metabolism parameters associated with not measuring α_R directly. Daytime ER was 54–340% higher than nighttime ER using $\delta^{18}O_{O_2}$, but diel ER parameter estimates were highly uncertain relative to traditional estimates of ecosystem metabolism. Diel variations in water temperature only accounted for 4–55% of the range of diel ER calculated using diel $\delta^{18}O_{O_2}$. Measured benthic flow chamber α_R varied within the range of literature values: from 0.9755 to 0.9954. Metabolism parameter estimates were very sensitive to choice of α_R within the measured and published range of values. The mean and uncertainty of diel ER estimates increased with decreasing α_R, with daily ER more than ten times higher given an α_R of 0.975 vs. 0.999. Diel changes in ER can be modeled using $\delta^{18}O_{O_2}$ and O_2, but diel ER estimates depend on the choice of α_R, suggesting the need to better understand how α_R may vary within spatial and temporal scales appropriate for $\delta^{18}O_{O_2}$ metabolism models.

Gross primary production (GPP) and ecosystem respiration (ER) govern the production, transformation, and retention of organic carbon (C) and nutrients in ecosystems. Accurate measurements of GPP and ER are needed in order to understand the metabolic balance and contributions of ecosystems to the global C cycle, but ER is still one of the largest gaps in our understanding of how freshwater ecosystems process C (del Giorgio and Williams 2005).

Scientists make two assumptions to simplify C cycling measurements in aquatic ecosystems. The first is that measurements of dissolved oxygen (O_2) can be used as a proxy for C cycling (Odum 1956). Most C cycling measurements in freshwater ecosystems are made using O_2, which is easier to measure than dissolved inorganic C but may not always accurately assess CO_2 fixation and ER (del Giorgio and Williams 2005). Production of O_2 may not occur in a 1 : 1 stoichiometric ratio with CO_2 fixation because O_2 can be evolved by both the Mehler reaction and photorespiration during periods of high light intensity (Mehler and Brown 1952; Brown 1953; Jackson and Volk 1970). While the relative contributions of the Mehler reaction and photorespiration to total O_2 cycling may be low, if these processes are responsible for increased O_2 cycling, the use of O_2 as a proxy for C cycling measurements may not be accurate.

The second assumption is that ER measured at night is equal to ER during the day and can therefore be applied to daytime changes in C and O_2 to isolate the contributions of GPP during the day. Daytime rates of ER are likely higher than nighttime rates (Tobias et al. 2007) due to increasing water temperatures, algal photosynthate exudation, and/or photo-breakdown of complex organic C. Water temperatures increase during the daytime and may raise the metabolic rates of organisms, thereby increasing O_2 consumption (Perkins et al. 2012). Algal exudation of dissolved organic C (DOC) and other photosynthates could enhance the availability of organic matter and subsequently increase daytime heterotrophic respiration (Cole et al. 1982; Kaplan and Bott 1982; Baines and Pace 1991). Complex DOC structures exposed to sunlight can break down into smaller molecular structures ("photo-breakdown"), potentially providing additional labile DOC for microbial growth and respiration during the day (Moran and Zepp 1997; De Lange et al. 2003; Amado et al. 2006).

$\delta^{18}O_{O_2}$ values represent a promising tool with which to measure diel rates of ER in aquatic ecosystems. Stable isotopes of oxygen can be used to measure ER without the influence of GPP during the day, and they provide an additional measured value when solving for unknown metabolism parameters. Three stable isotopes of oxygen exist naturally: Oxygen-16 (^{16}O) is very common, while oxygen-17 (^{17}O) and oxygen-18 (^{18}O) are less abundant. Respiration discriminates against $^{18}O_{O_2}$, leaving behind a greater fraction of ^{18}O than ^{16}O dissolved in the water (Luz and Barkan 2000). Photosynthesis lowers $\delta^{18}O_{O_2}$ values by producing O_2 with similar $\delta^{18}O_{O_2}$ values as source H_2O (Kroopnick 1975). This discrimination during respiration allows scientists to infer increased O_2 consumption during the day if there is a greater ratio of $^{18}O_{O_2}$: $^{16}O_{O_2}$ left behind in the water after accounting for photosynthesis (Bender et al. 1987; Luz et al. 2002; Tobias et al. 2007).

Estimates of ER using $\delta^{18}O_{O_2}$ values in lake and marine ecosystems suggest that O_2 consumption is up to tenfold

* Corresponding author: ehotchkiss@gmail.com

[a] Present address: Department of Ecology and Environmental Science, Umeå University, Umeå, Sweden

higher during daytime than at night (Bender et al. 1987; Luz et al. 2002). Because of the link between biological processes and $\delta^{18}O_{O_2}$ values, scientists have monitored changes in $\delta^{18}O_{O_2}$ values over diel cycles in streams and rivers (Parker et al. 2010), and some have estimated ecosystem metabolism from these diel changes (Tobias et al. 2007; Venkiteswaran et al. 2007; Holtgrieve et al. 2010). While $\delta^{18}O_{O_2}$ values can provide an additional set of data with which to estimate daily rates of GPP and ER (Holtgrieve et al. 2010), few studies have used diel changes in $\delta^{18}O_{O_2}$ values to estimate diel changes in ER in streams and rivers. One notable exception is Tobias et al. (2007), who found that daytime ER, measured using $\delta^{18}O_{O_2}$, was sometimes more than twice as great as nighttime ER.

Calculations of GPP and ER using $\delta^{18}O_{O_2}$ values may be sensitive to the choice of α_R (the respiration fractionation factor), which represents the fractionation against $^{18}O_{O_2}$ during respiration. Pelagic water-column measurements of α_R range from 0.975 to 1.015 and vary by site, organism, and season (Lane and Dole 1956; Kiddon et al. 1993; Wang et al. 2008), limiting the use of $\delta^{18}O_{O_2}$ for ecosystem metabolism calculations. Although Tobias et al. (2007) quantified α_R in static incubations that included benthic substrates, α_R in flowing waters has not been quantified, which also limits the use of $\delta^{18}O_{O_2}$ values in stream and river ecosystem metabolism calculations.

In this paper, we test current assumptions about ecosystem metabolism and quantify the discrimination against $^{18}O_{O_2}$ in flowing waters to improve estimates of diel ER. We used a combination of whole-stream and flow-chamber measurements, linked with Bayesian inverse modeling, to answer the following questions: (1) How much greater is daytime ER than nighttime ER, measured as O_2, in streams? (2) How do estimates of diel O_2 consumption from $\delta^{18}O_{O_2}$ models compare to estimates from temperature-driven O_2 models? (3) How sensitive are estimates of ER to the respiration fractionation factor required for $\delta^{18}O_{O_2}$ metabolism models? We estimated diel changes in ER using measurements of O_2, light, temperature, and $\delta^{18}O_{O_2}$ to test the hypothesis that ER varies over 24 h cycles. We measured the fractionation factor for respiration in dark benthic flow-through chambers. We compared diel ER rates to those calculated using temperature-adjusted ER calculations to quantify the potential underestimation of total ER in streams, and we quantified the uncertainty of GPP, ER, and α_R estimates using Bayesian inverse modeling.

Methods

Site descriptions—We measured reach-scale diel changes in O_2, $\delta^{18}O_{O_2}$, and water temperature in three open-canopy streams in central and western Wyoming to calculate ecosystem metabolism. Kelly Warm Springs (Kelly; 43°38′24.51″N, 110°37′5.65″W) and Polecat Creek (Polecat; 44°6′37.82″N, 110°41′21.11″W) are both highly productive spring streams with warm groundwater inputs in Grand Teton National Park, Wyoming. Red Canyon Creek (Red Canyon; 42°40′48.76″N, 108°39′53.35″W) is a less productive second-order stream south of Lander, Wyoming. We collected diel data from Red Canyon, Polecat, and Kelly on 24–25 June 2007, 20–21 July 2007, and 27–28 July 2007, respectively. We used dark flow-through chambers to estimate the fractionation factor for respiration (α_R) during July 2009 in Kelly and Ditch Creek, Wyoming (Ditch; 43°39′48.39″N, 110°37′52.47″W). Ditch Creek was chosen as the second site for α_R measurements because it was near Kelly and less productive than Kelly and Polecat.

Data collection—We measured diel changes in O_2, water temperature (T), light, $\delta^{18}O_{O_2}$, and $\delta^{18}O_{H_2O}$ at each site. We placed Hydrolab Minisondes equipped with Clark-type membrane electrodes and stirrers (Hach Environmental) at one (Kelly) or two (Red Canyon and Polecat) locations in each stream reach to measure diel changes in O_2 and T at 10 min intervals for 24–48 h periods. Red Canyon and Polecat sites 1 and 2 were upstream and downstream, respectively. We measured and modeled date- and site-specific photosynthetic photon flux density (PPFD; μmol m^{-2} s^{-1}) at 10 min intervals for the same date and time period as our O_2 and $\delta^{18}O_{O_2}$ measurements (Yard et al. 2005). We collected 12 mL of dissolved water every 4 h for a 28 h period and preserved samples with $HgCl_2$ for $\delta^{18}O_{O_2}$ analyses (Thermo Finnigan Gas Bench to Delta Plus XP mass spectrometer). We also collected and preserved water samples for site-specific $\delta^{18}O_{H_2O}$ measurements (Thermo Finnigan Gas Bench to Delta Plus XP mass spectrometer).

We measured and modeled air–water gas exchange and physical parameters for each site. We calculated gas-exchange rates (K_{O_2}; d^{-1}) for each stream reach using additions of sulfur hexafluoride (SF_6), a biologically inert gas that evades at rates proportional to O_2 (Wanninkhof 1992; Cole and Caraco 1998). We also solved for K_{O_2} as an unknown parameter for Red Canyon sites. We converted measured K_{SF_6} to K_{600} and K_{O_2} using temperature and gas-specific Schmidt numbers and the relationship between K values and Schmidt numbers (Jähne et al. 1987; Wanninkhof 1992). We added salt as a conservative tracer with SF_6 additions to estimate groundwater dilution downstream. We measured stream width (w; m) at 20 sites within each stream reach. We measured velocity (v; m min^{-1}) at 10 transects within our study reach using a Marsh McBirney flow meter. We used measurements of stream width and velocity to calculate discharge (Q; m^3 min^{-1}), and estimated the mean depth (z; m) from width, velocity, and discharge: $z = \frac{Q}{w \times v}$.

Ecosystem metabolism: Diel O_2 model—GPP and ER can be calculated using a one-station, open-channel metabolism model (Odum 1956), where the change in dissolved O_2 concentrations (g O_2 m^{-3}) between measurement intervals (t and $t-1$) is a function of ER, GPP, air–water gas exchange (K_{O_2}), and the time between measurement intervals (Δt; d):

$$O_{2_{(t)}} = O_{2_{(t-1)}} + \left(\frac{GPP}{z} + \frac{ER}{z} + K_{O_2} \left(O_{2_{sat(t-1)}} - O_{2_{(t-1)}} \right) \right) \Delta t \quad (1)$$

where GPP is a positive rate of O_2 production (g O_2 m^{-2} d^{-1}), ER is a negative rate of O_2 consumption (g O_2

Table 1. Model parameter symbols, descriptions, sources, and units.

Parameter symbol	Parameter description	Source	Units
O_2	Dissolved oxygen	Measured	g O_2 m^{-3}
$O_{2_{sat}}$	O_2 at saturation	Modeled	g O_2 m^{-3}
K_{O_2}	O_2 gas-exchange rate	Measured and modeled	d^{-1}
PPFD	Photosynthetic photon flux density	Estimated (Yard et al. 2005)	μmol m^{-2} s^{-1}
ER	Ecosystem respiration	Modeled	g O_2 m^{-2} d^{-1}
ER_{base}	Baseline ER without dielMET added	Modeled	g O_2 m^{-2} d^{-1}
GPP	Gross primary production	Modeled	g O_2 m^{-2} d^{-1}
GPP_{base}	Baseline GPP without dielMET added	Modeled	g O_2 m^{-2} d^{-1}
dielMET	Diel metabolism term	Modeled	g O_2 m^{-2} d^{-1}
Δt	Time step between measurements	Measured	d
z	Mean stream depth	Measured	m
T	Water temperature	Measured	°C
$\delta^{18}O_{O_2}$	$\delta^{18}O$ value of dissolved O_2	Measured	‰ vs. VSMOW
$\delta^{18}O_{H_2O}$	$\delta^{18}O$ value of H_2O	Measured	‰ vs. VSMOW
$^{18}O_{O_2}$	Concentration of ^{18}O in dissolved O_2	Measured	g ^{18}O m^{-3}
AF_{DO}	Atomic fraction of dissolved O_2	Measured	mol ^{18}O : mol O_2
AF_w	Atomic fraction of H_2O	Measured	mol ^{18}O : mol O_2
AF_{atm}	Atomic fraction of atmospheric air	Literature	mol ^{18}O : mol O_2
α_g	Fractionation factor: air–water gas exchange	Literature	—
α_s	Fractionation factor: O_2 dissolution in H_2O	Literature	—
α_R	Fractionation factor: respiration	Measured, modeled, and literature	—
α_p	Fractionation factor: photosynthesis	Literature	—
ε_R	Enrichment factor: respiration	Measured, modeled, and literature	—

m^{-2} d^{-1}), z is mean stream depth (m), and K_{O_2} is the O_2 gas-exchange rate (d^{-1}). O_2 saturation ($O_{2_{sat(t)}}$; g O_2 m^{-3}) is calculated using water temperature (T; °C) and barometric pressure (BP; mm Hg) for each measurement time (t; as in Hotchkiss and Hall 2010). All parameter descriptions and units are listed in Table 1.

Various expansions of the simple O_2 model in Eq. 1 have been used to better constrain unknown values of GPP, ER, and K (Hanson et al. 2008; Holtgrieve et al. 2010). Many expanded metabolism models use light and/or temperature to improve model estimates of GPP and ER. Light-driven GPP calculations can use a light saturation photosynthesis–irradiance curve or a linear photosynthesis–irradiance relationship (Van de Bogert et al. 2007; Hanson et al. 2008; Holtgrieve et al. 2010):

$$O_{2_{(t)}} = O_{2_{(t-1)}} + \left(\frac{GPP}{z} \times \frac{PPFD_{(t-1)}}{\sum PPFD_{24\,h}}\right) + \frac{ER \times \Delta t}{z} + K_{O_2} \times \Delta t \times \left(O_{2_{sat(t-1)}} - O_{2_{(t-1)}}\right) \quad (2)$$

We used this model to obtain prior daily estimates of base GPP and base ER modeled from O_2 alone (see "Bayesian estimation of parameters" section). We used site-specific estimates of BP measured with a Hydrolab Surveyor (Hach Environmental). We modeled O_2 using measured K_{O_2} for Kelly and Polecat and modeled K_{O_2} for Red Canyon. We measured minimal groundwater intrusion based on conservative solute additions, so we did not include groundwater estimate corrections in any of our metabolism models.

We also used a temperature-driven O_2 metabolism model to compare diel rates of ER estimated with diel temperature vs. $\delta^{18}O_{O_2}$. Temperature-driven ER calculations often use the van't Hoff–Arrhenius equation (as in Venkiteswaran et al. 2007; Holtgrieve et al. 2010):

$$ER_t = ER_{T_{fix}} \times 1.047^{(T_t - T_{fix})} \quad (3)$$

where rates of O_2 consumption at different water temperatures (T) are extrapolated from ER estimated at a known temperature ($ER_{T_{fix}}$; often 20°C or temperature at nighttime).

Ecosystem metabolism: Diel $\delta^{18}O_{O_2}$ model—Ecosystem metabolism can also be calculated using the changes in $\delta^{18}O_{O_2}$ and O_2, where concentrations of $^{18}O_{O_2}$ are modeled as a function of isotope values of sources, isotope fractionation values, air–water gas exchange, ER, and GPP (modified from Tobias et al. 2007; parameter descriptions and units are in Table 1):

$$^{18}O_{O_2(t)} = {}^{18}O_{O_2(t-1)} + \left(\frac{GPP}{z} \times \alpha_p \times AF_w \times \Delta t\right) + \left(\frac{ER}{z} \times \alpha_R \times AF_{DO(t-1)} \times \Delta t\right) + \left(K_{O_2} \times \alpha_g \times \Delta t \times \left(\left(O_{2_{sat(t-1)}} \times \alpha_s \times AF_{atm}\right) - {}^{18}O_{O_2(t-1)}\right)\right) \quad (4)$$

Similar to the O_2 metabolism models above, time-specific estimates for $^{18}O_{O_2}$ are a function of $^{18}O_{O_2}$, GPP, ER, air–water gas exchange, and the isotope fractionation factors and source values of the atomic fraction of ^{18}O

specific to H_2O (AF_w), dissolved O_2 (AF_{DO}), and atmospheric O_2 (AF_{atm}). Fractionation factors describe the enrichment of $^{18}O_{O_2}$ due to air–water gas exchange (α_g = 0.9972), air dissolution in water (α_s = 1.0007), respiration (α_R; varied by site measurement and within range of literature values), and photosynthesis (α_p = 1.0000). We converted sample and literature values to $^{18}O_{O_2}$ concentrations and atomic fractions (AF) used in Eq. 4. The value of $\delta^{18}O_{O_2}$ was calculated using the isotopic ratio of a sample relative to the isotopic ratio of Vienna standard mean ocean water (R_{VSMOW} = 1.008; Craig 1961), where:

$$R_{VSMOW} = \frac{^{18}O}{^{16}O} \tag{5}$$

$$\text{Sample } \delta^{18}O_{O_2} = \left(\frac{R_{sample}}{R_{VSMOW}} - 1\right) \times 1000 \tag{6}$$

Atomic fractions (AF) were calculated from R_{sample} as:

$$AF = \frac{R}{1-R} \tag{7}$$

and the concentration of samples ($^{18}O_{O_2}$) was calculated as:

$$^{18}O_{O_2} = AF \times O_2 \tag{8}$$

To model diel ER, we introduced an additional parameter that increased total ER and GPP by the same amount during the day to account for the equal consumption and production of O_2 not accounted for with net measurements of diel O_2. We added a new diel metabolism parameter, dielMET, to the dual O_2 and $\delta^{18}O_{O_2}$ model to reflect additional changes in diel metabolism not detectable from O_2 data alone. Having diel $\delta^{18}O_{O_2}$ in addition to O_2 data allowed us to solve for not only base GPP and ER (hereafter, GPP_{base} and ER_{base}), but also dielMET. By adding the dielMET parameter, we assumed diel measurements of dissolved O_2 reflected the net diel changes in O_2 due to GPP, ER, and air–water gas exchange. To secure the mass balance of measured diel O_2, we added dielMET to GPP_{base} and subtracted dielMET from ER_{base}. Thus, total rates of GPP and ER are equal to GPP_{base} or ER_{base} (GPP and ER in traditional O_2 models above and GPP_{base} and ER_{base} in Eqs. 9a and 9b below) plus or minus dielMET, respectively.

We solved for unknown parameters GPP_{base}, ER_{base}, and dielMET using Bayesian inverse modeling (described below). We modified the Tobias et al. (2007) and Holtgrieve et al. (2010) $\delta^{18}O_{O_2}$ metabolism models in three ways: (1) We simultaneously inversely modeled O_2 and $^{18}O_{O_2}$ concentrations at 10 min intervals by including a separate O_2 model (Eq. 9a) in our inverse modeling framework with shared GPP_{base} and ER_{base} between the two models; (2) we updated Eq. 4 with a dielMET parameter to solve for diel changes in total ER as informed by diel changes in $\delta^{18}O_{O_2}$ and light intensity (Eq. 9b); and (3) we used one-station O_2 metabolism (Eq. 2) means and credible interval estimates for GPP and ER as prior distribution inputs for GPP_{base} and ER_{base} in the dual O_2 and $\delta^{18}O_{O_2}$ model.

$$O_{2(t)} = O_{2(t-1)} + \left(\frac{GPP_{base}}{z} \times \frac{PPFD_{(t-1)}}{\sum PPFD_{24\,h}}\right) + \left(\frac{ER_{base} \times \Delta t}{z}\right) + \left(K_{O_2} \times \left(O_{2_{sat(t-1)}} - O_{2_{(t-1)}}\right) \times \Delta t\right) \tag{9a}$$

$$^{18}O_{O_2(t)} = {}^{18}O_{O_2(t-1)} + \left(\frac{(GPP_{base} + dielMET)}{z} \times \frac{PPFD_{(t-1)}}{\sum PPFD_{24\,h}} \times \alpha_p \times AF_w\right) + \left(\frac{ER_{base} \times \Delta t}{z} \times \alpha_R \times AF_{DO}(t-1)\right) + \left(\frac{(-dielMET)}{z} \times \frac{PPFD_{(t-1)}}{\sum PPFD_{24\,h}} \times \alpha_R \times AF_{DO(t-1)}\right) + \left(K_{O_2} \times \alpha_g \times \Delta t \times \left(\left(O_{2_{sat(t-1)}} \times \alpha_s \times AF_{atm}\right) - {}^{18}O_{O_2(t-1)}\right)\right) \tag{9b}$$

Diel $\delta^{18}O_{O_2}$ data allowed us to estimate diel changes in total GPP and ER (via dielMET) that O_2, temperature, and light data cannot predict. This model structure allowed us to test the assumption that daytime ER was greater than nighttime ER using diel $\delta^{18}O_{O_2}$ data, and acknowledge that if daytime ER is greater than nighttime ER, then daytime GPP must also be larger than GPP measured with O_2 to keep diel modeled concentrations of O_2 the same as measured O_2.

We linked dielMET to light as with GPP. This dual model assumed that diel changes in total GPP and ER could be explained by diel changes in PPFD to avoid creating an overfitted $\delta^{18}O_{O_2}$ model with exact solutions of total ER based on $ER_{20°C}$ and T (Eq. 3). Because we had 10 min measurement intervals for O_2, PPFD, and T but approximately 4 h intervals between $\delta^{18}O_{O_2}$ measurements, we modeled O_2 and $^{18}O_{O_2}$ concentrations on 10 min intervals (t = 0.00694 d). We only compared our modeled O_2 and estimates and calculated joint likelihoods for O_2 and $\delta^{18}O_{O_2}$ models at the approximately 4 h $\delta^{18}O_{O_2}$ measurement intervals (t = 0.16667 d).

Bayesian estimation of parameters—We used inverse modeling and Bayesian parameter estimation to solve for GPP_{base}, ER_{base}, and dielMET (similar to Holtgrieve et al. 2010). This approach estimates the probability distribution of unknown parameters that produce the best fit between the modeled and measured O_2 data and does not rely on O_2 data to directly solve for GPP and ER, as have past exact solution methods (Mulholland et al. 2001; Hotchkiss and Hall 2010). Bayesian parameter estimation also allows for the inclusion of prior information about parameters, where the joint posterior probability of all parameter estimates (GPP, ER, others) given the data (O_2) is proportional to the product of the metabolism model likelihood ($\mathcal{L}$) and prior probability distributions for unknown parameters (Holtgrieve et al. 2010). Posterior probability distribution estimates were based on the Bayes rule (Hilborn and Mangel 1997):

$$\text{Probability}(\theta|D) \propto \mathcal{L}(D|\theta) \times \text{Prior}(\theta) \tag{10}$$

where the posterior probability of the parameter estimates (θ) was calculated as the product of the joint probabilities of modeled O_2 and $^{18}O_{O_2}$ based on O_2 and $^{18}O_{O_2}$ data (D), multiplied by prior information about the mean and distribution of GPP_{base}, ER_{base}, and dielMET parameters (θ). Likelihood calculations assumed normally distributed (N) error:

$$\mathcal{L}(D|\theta) = \prod_{i=1}^{n} N\left(D_i|\mu_i,\sigma_i^2\right) \quad (11)$$

where the likelihood of D given θ is the product of the likelihoods of D for i to n measurements given modeled oxygen concentrations (μ_i) and variance (σ_i^2). We used a "random walk" Metropolis algorithm and Markov chain Monte Carlo (MCMC) to simulate the posterior distribution of unknown parameters using the R *metrop* function in the *mcmc* package (Geyer and Johnson 2013; R Development Core Team 2012). Each model was run for at least 200,000 iterations using three different starting values within our prior distributions to ensure convergence on the same posterior parameter estimate. We altered the proposed distribution step size to obtain an acceptance rate near 20% (Geyer and Johnson 2013) and subtracted the first 10,000 iterations of burn-in time based on visual assessments of MCMC chain behavior before calculating parameter posterior distribution means and credible intervals. We did not thin MCMC chains.

The Bayesian modeling framework requires prior information about the distribution of GPP_{base}, ER_{base}, and dielMET as well as potential error in O_2 and $\delta^{18}O_{O_2}$ estimates. We estimated O_2 and $\delta^{18}O_{O_2}$ error terms as unknown parameters with priors of the mean and range of O_2 and $\delta^{18}O_{O_2}$ data (used to calculate likelihood; Eq. 10) as the variance of measured O_2 and $\delta^{18}O_{O_2}$. O_2 model priors for GPP and ER were minimally informative normal distributions with standard deviations beyond probable rates of GPP and ER for Wyoming streams. We used O_2 model posterior distribution estimates of GPP and ER as prior distributions for GPP_{base} and ER_{base} in the $\delta^{18}O_{O_2}$ model. Because we had little prior information about dielMET, we used minimally informative uniform distributions (0 to 100 g O_2 m^{-2} d^{-1}) as prior probability distributions for dielMET in $\delta^{18}O_{O_2}$ models.

We generated two sets of model outputs to compare temperature-adjusted O_2 model estimates of GPP and ER (Eqs. 2 and 3) with total GPP and ER (calculated from model output of dielMET, GPP_{base}, and ER_{base}) from the dual O_2 and $\delta^{18}O_{O_2}$ model (Eqs. 9a and 9b). Data input for both models included diel PPFD and T. Fixed parameters were BP, t, K, and z, and K_{O_2} was adjusted for diel changes in T. We also fixed all fractionation factors and AF of source water and the atmosphere in the dual O_2 and $\delta^{18}O_{O_2}$ model for this comparison. Diel O_2 and $\delta^{18}O_{O_2}$ data were only used to calculate the likelihood of parameter estimates (Eq. 11).

Respiration fractionation factor for $\delta^{18}O_{O_2}$ in flowing waters—To compare fractionation factors in flowing benthic chambers with literature values for static water and sediment incubations, we measured the fractionation factor for composite dark O_2 consumption in four replicate dark 4.2 liter circulating flow chambers in Kelly and Ditch. We placed stream rocks in the base of the flow chambers, sealed the chambers under water to remove all air bubbles, covered the chambers with multiple layers of black plastic, and incubated the sealed dark chambers in situ for 6 to 7 h at each site (long enough to ensure substantial O_2 depletion but without inducing anoxia). We measured O_2 and $\delta^{18}O_{O_2}$ at the start and the end of the dark flow-through incubations and calculated the site-specific enrichment factors (ε_R) and fractionation factors (α_R) for respiration (using relationships between ε_R, $\delta^{18}O_{O_2}$, and O_2 from the Rayleigh equation as in Tobias et al. 2007), where

$$\varepsilon_R \times \ln(f_{DO}) = \delta^{18}O_{O_{2(t)}} - \delta^{18}O_{O_{2(t-1)}} \quad (12)$$

$$\alpha_R = 1 + \frac{\varepsilon_R}{1000} \quad (13)$$

ε_R was calculated from the fraction of the original dissolved O_2 remaining in the chamber water (f_{DO}) at the end of each incubation and the change in $\delta^{18}O_{O_2}$ between the start ($\delta^{18}O_{O_{2(t-1)}}$) and end ($\delta^{18}O_{O_{2(t)}}$) of each incubation (similar to static benthic incubations by Tobias et al. 2007 and static bottle incubations by Quay et al. 1995; Helman et al. 2005).

We used fixed measurements of α_R to estimate dielMET and ER_{base} in our three study streams. We compared $\delta^{18}O_{O_2}$ model dielMET and ER_{base} estimates and uncertainty when we fixed measured α_R, fixed a range of commonly used literature values for α_R, or included α_R as an unknown parameter with prior probability distributions based on measured or literature values.

Results

Ecosystem metabolism: Diel O_2 model—O_2 varied over 24 h at all sites, corresponding to greater rates of GPP and ER (Eq. 2; Fig. 1). All streams were heterotrophic: Rates of ER exceeded GPP at all sites. Daily rates of GPP were greatest in Kelly and lowest in both Red Canyon sites (Table 2). Daily rates of ER were greatest in Kelly and lowest in Polecat site 1 and Red Canyon site 2 (Table 2). Posterior probability estimates of GPP and ER were well constrained and provided good fits of modeled O_2 to O_2 data (Fig. 1). We used the posterior distributions for GPP and ER from O_2 models (Eq. 2) as the prior probability distributions for GPP_{base} and ER_{base} in $\delta^{18}O_{O_2}$ models (Eqs. 9a and 9b).

Ecosystem metabolism: Diel $\delta^{18}O_{O_2}$ model—Posterior probability distributions of GPP_{base} and ER_{base} in the $\delta^{18}O_{O_2}$ model were similar to the priors from the O_2-based model at each site. The magnitude of diel $\delta^{18}O_{O_2}$ cycles varied by site, with large diel changes in Kelly and Polecat and small diel changes in Red Canyon (Fig. 1). All $\delta^{18}O_{O_2}$ parameter estimates converged on a nonzero dielMET term (Table 2). The $\delta^{18}O_{O_2}$ model posterior dielMET estimates reflected the magnitude of diel $\delta^{18}O_{O_2}$ and O_2: Estimated

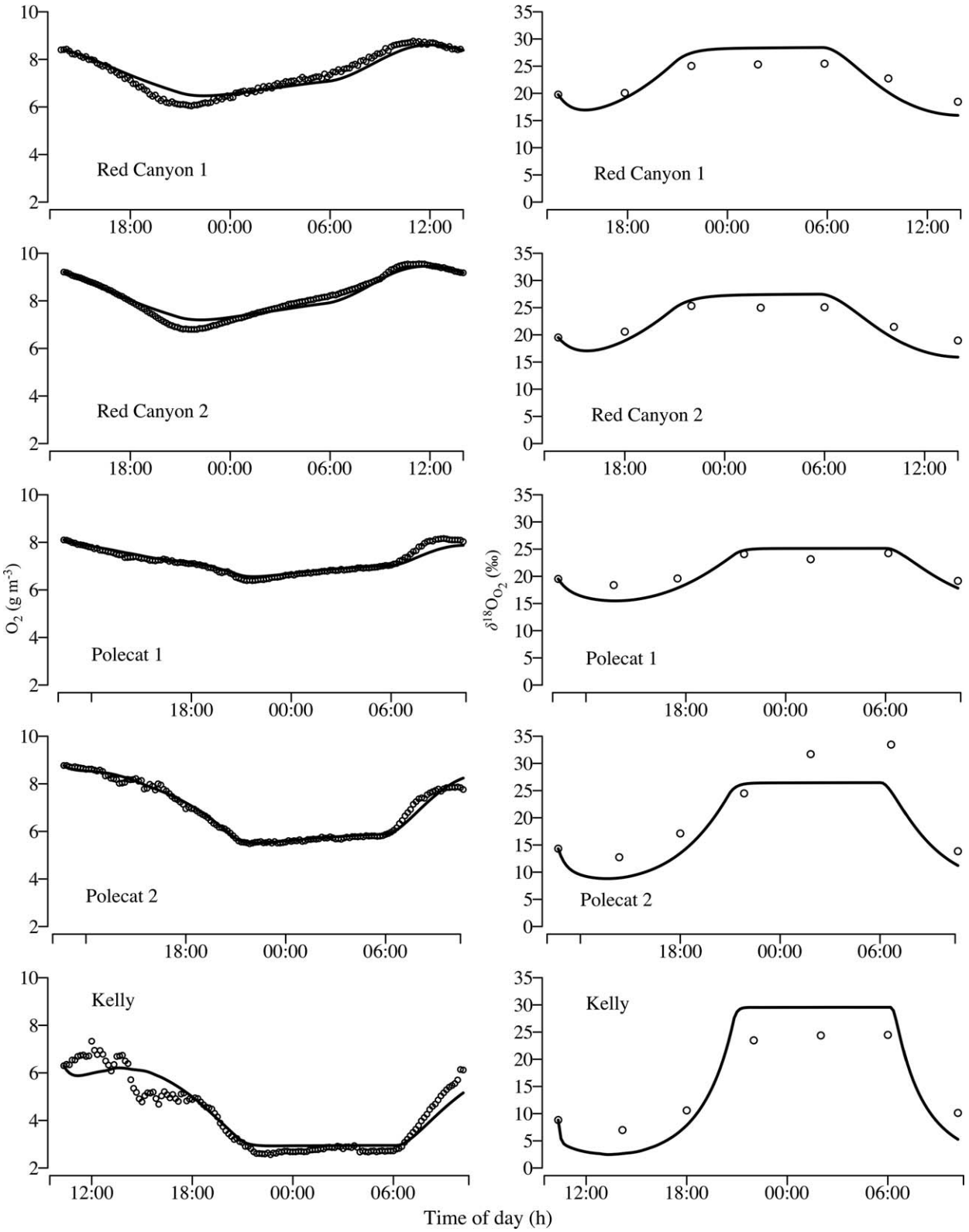

Fig. 1. Measured vs. modeled O_2 and $\delta^{18}O_{O_2}$ during 24 h sampling periods in three Wyoming streams during summer 2007. Measured O_2 and $\delta^{18}O_{O_2}$ data are noted with open circles; solid lines represent estimates of O_2 and $\delta^{18}O_{O_2}$ using a Bayesian inverse metabolism modeling framework (Eqs. 9a and 9b).

Table 2. Parameter estimates and 2.5–97.5% credible intervals (CI) for gross primary production (GPP), ecosystem respiration (ER), and a modeled diel metabolism term (dielMET) using flow-through chamber measurements of the fractionation against ^{18}O during respiration (α_R). Kelly parameters were estimated using measured α_R in Kelly ($\alpha_R = 0.9884$). Red Canyon and Polecat parameters were estimated using the mean α_R measured in Kelly and Ditch ($\alpha_R = 0.9852$). Diel GPP and ER from the $^{18}O_{O_2}$ model were calculated as GPP_{base} + dielMET and ER_{base} + (−dielMET), respectively. All units are g O_2 m^{-2} d^{-1}.

	GPP_{base}		ER_{base}		DielMET		Diel GPP	Diel ER
Site	Mean	CI	Mean	CI	Mean	CI	Mean	Mean
Kelly	14.9	14.3, 15.4	−38.6	−39.3, −37.8	48.8	35.4, 65.2	63.7	−87.4
Red Canyon 1	2.5	2.4, 2.6	−9.3	−9.4, −9.2	3.7	2.5, 5.0	6.2	−12.9
Red Canyon 2	2.4	2.4, 2.5	−6.7	−6.7, −6.6	2.8	1.9, 3.7	5.2	−9.4
Polecat 1	5.1	4.9, 5.3	−5.5	−5.7, −5.2	3.1	2.1, 4.2	8.2	−8.5
Polecat 2	11.5	11.4, 11.7	−13.2	−13.3, −13.0	8.8	1.7, 15.9	20.3	−22.0

dielMET in Kelly was quite high, with lower dielMET estimates for Polecat and Red Canyon, respectively. Estimated rates of dielMET in Kelly more than doubled the diel rates of GPP and ER throughout the day (Table 2).

Comparing diel O_2 and $\delta^{18}O_{O_2}$ estimates of ER—Temperature-driven O_2 and dielMET $\delta^{18}O_{O_2}$ models both estimated diel changes in ER for all three streams (Table 3; Fig. 2). ER was greater during the day than night at all sites for all models (Fig. 2). The light- and temperature-adjusted O_2 metabolism model accounted for only a small fraction of the increased daytime ER calculated using $\delta^{18}O_{O_2}$, especially at the most productive site (Kelly), suggesting that something else, in addition to temperature, increased rates of O_2 cycling during the daytime. Kelly maximum daytime ER was 410% greater than the maximum rate of ER estimated using the temperature-adjusted O_2 model. The ranges of diel ER rates over one 24 h period were 80–2400% greater using $\delta^{18}O_{O_2}$ model ER estimates compared to temperature-adjusted O_2 model estimates (Table 3; Fig. 2).

Respiration fractionation factor for $\delta^{18}O_{O_2}$ in flowing waters—The mean flow-through benthic chamber measurements of α_R for Kelly and Ditch were within the range of values reported in the literature (Fig. 3). Mean measured α_R was slightly larger in Kelly (0.9884; standard deviation [SD] = 0.0084) than α_R in Ditch (0.9821; SD = 0.0038) and reported from static chambers in the literature. Posterior estimates of dielMET (and thus, total ER) were very sensitive to variation in α_R, even within the range of measured (this study) and published α_R values (Fig. 4). Posterior parameter estimates of dielMET and α_R did not converge on a constrained estimate when we included α_R as an unknown parameter (with prior) in the $\delta^{18}O_{O_2}$ metabolism model, so total ER estimates presented in Fig. 4 are from a range of fixed α_R values. Mean Kelly dielMET estimates ranged from 12.2 to 95.5 g O_2 m^{-2} d^{-1} across the high to low range of α_R, respectively. Increasing values of α_R decreased mean dielMET estimates, with dielMET estimates near zero when $\alpha_R = 1.0$. Varying α_R also changed the confidence in dielMET estimates: Credible intervals were largest at low α_R values. Larger values of α_R produced ER estimates with smaller credible intervals (Fig. 4).

Table 3. A comparison of mean, minimum, and maximum ecosystem respiration (ER) from temperature-driven O_2 (Eqs. 2 and 3) and dielMET $^{18}O_{O_2}$ (Eqs. 9a and 9b) metabolism models. Diel ER from the dielMET $^{18}O_{O_2}$ model was calculated as ER_{base} + (−dielMET). All units are g O_2 m^{-2} d^{-1}.

		Diel ER		
Site	Model	Mean	Min	Max
Kelly	Temperature O_2	−29.8	−27.8	−33.0
	DielMET $^{18}O_{O_2}$	−87.4	−38.3	−168.6
Red Canyon 1	Temperature O_2	−10.0	−7.7	−12.8
	DielMET $^{18}O_{O_2}$	−12.9	−9.3	−18.6
Red Canyon 2	Temperature O_2	−7.4	−5.8	−9.6
	DielMET $^{18}O_{O_2}$	−9.4	−6.7	−13.7
Polecat 1	Temperature O_2	−6.7	−5.6	−8.3
	DielMET $^{18}O_{O_2}$	−8.5	−5.7	−13.6
Polecat 2	Temperature O_2	−14.1	−11.6	−18.0
	DielMET $^{18}O_{O_2}$	−22.0	−13.2	−35.9

Discussion

Drivers of high daytime O_2 cycling—Daytime ER was greater than nighttime ER in three Wyoming streams. Most ecosystem metabolism measurements using only O_2 are limited to estimates of ER based on the assumption that nighttime ER is the same as daytime ER or that ER varies according to laboratory-derived temperature–respiration relationships. We estimated time-varying rates of diel ER using diel measurements of O_2 coupled with $\delta^{18}O_{O_2}$. While several studies have measured diel changes in $\delta^{18}O_{O_2}$, used these data to calculate daily rates of GPP and ER, and noted the role of diel changes in GPP and ER in driving these swings, few have used $\delta^{18}O_{O_2}$ to calculate diel changes in ER. The few studies that used $\delta^{18}O_{O_2}$ to estimate different rates of ER during the day and night (or in light and dark incubations) concluded that daytime (or light incubation) respiration may be up to tenfold greater than nighttime rates (Bender et al. 1987; Tobias et al. 2007).

We modeled dielMET as a function of light to estimate diel changes in GPP and ER beyond GPP_{base} and ER_{base} measured from diel changes from net O_2. Higher rates of daytime than nighttime respiration have been estimated

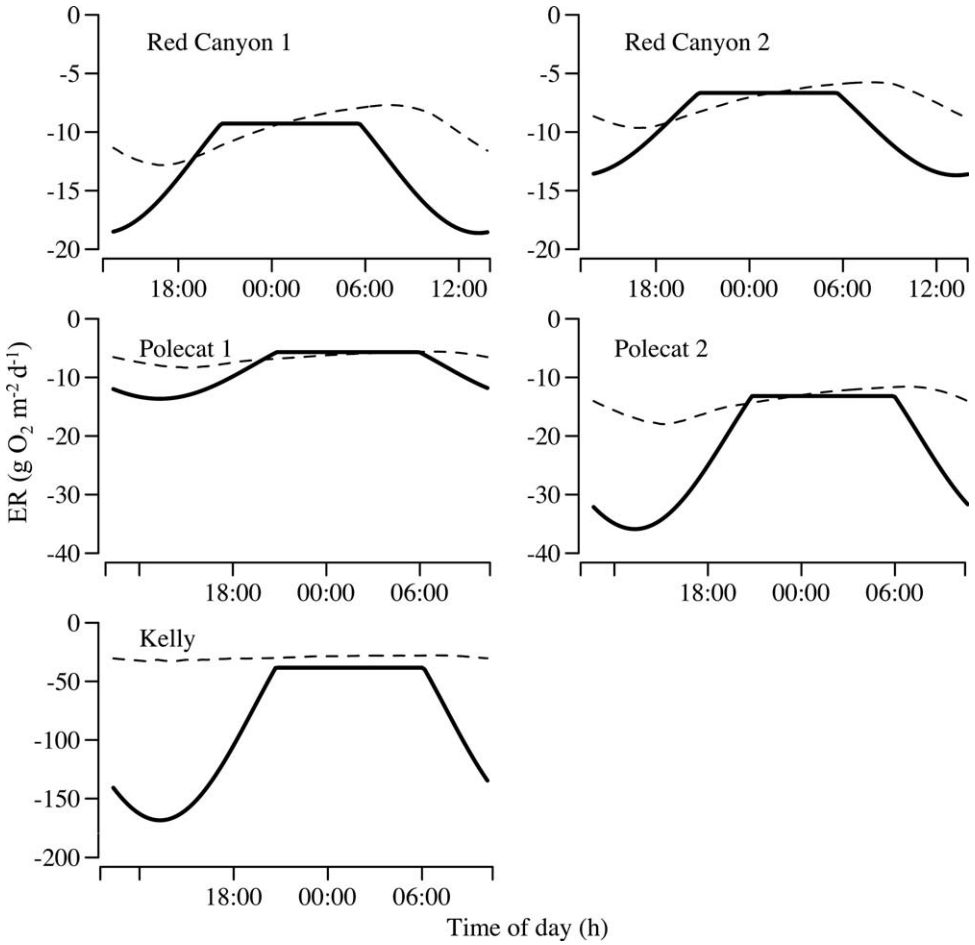

Fig. 2. Diel rates of ecosystem respiration (ER) in three Wyoming streams estimated using a temperature-adjusted O_2 metabolism model (dashed lines; Eqs. 2 and 3) and a dual O_2 and $\delta^{18}O_{O_2}$ metabolism model (solid lines; Eqs. 9a and 9b, where ER = ER_{base} + [−dielMET]).

using pulses of light in bottle incubations and by including light in ecosystem models. Instead of separating light and dark bottles and assuming constant respiration rates in light and dark, light pulse experiments estimate O_2 consumption in the dark immediately after a period of light exposure and assume that the immediate O_2 consumption rates reflect rates of light respiration (Weger et al. 1989; Pringault et al. 2007). Rates of light respiration measured by the light pulse technique for coastal plankton assemblages, marine diatoms, hypersaline mats, and intertidal sediments were 3–10 times greater than dark respiration (Weger et al. 1989; Epping and Jørgensen 1996; Pringault et al. 2007). At the stream reach scale, using light to model diel changes in O_2 produced a better fit of modeled and measured O_2 (Parkhill and Gulliver 1999). Diel changes in light intensity drive the mechanisms likely responsible for diel changes in ER measuring using O_2 and $\delta^{18}O_{O_2}$: light-mediated O_2 cycling, water temperature, GPP, and DOC availability.

Metabolism measurements using $\delta^{18}O_{O_2}$ assume that diel changes in $\delta^{18}O_{O_2}$ are a product of mitochondrial respiration and fully reflect an increase in biological C cycling. Other biotic and abiotic processes during the day also result in fractionation against $^{18}O_{O_2}$, including photorespiration (α = 0.979), the Mehler reaction (α = 0.985), alternative oxidase (α = 0.969), and photolysis (α = 0.988–0.995; Luz et al. 2002; Chomicki and Schiff 2008). Although likely less common than dark respiration, all of these processes discriminate against $^{18}O_{O_2}$. Our measurements of composite dark respiration fractionation excluded light reactions with fractionation against $^{18}O_{O_2}$ and may not fully reflect whole-stream diel $^{18}O_{O_2}$ dynamics. Luz et al. (2002) used ^{18}O and ^{14}C isotope tracers to compare O_2 and C cycling and estimate overall discrimination against $^{18}O_{O_2}$ in Lake Kinneret. Rates of O_2 production were about 7.5 times greater than C fixation, and models suggested the role of the alternative oxidase pathway, in addition to photorespiration, dark respiration, and/or the Mehler reaction, in driving changes in $\delta^{18}O_{O_2}$ (Luz et al. 2002). In another lake, coupled measurements of CO_2 and O_2 cycling using ^{13}C tracers found similar respiration rates, measured as CO_2 and O_2, at the ecosystem level (Carvalho and Eyre 2012). We suggest that O_2 light reactions only account for a small fraction of total O_2 cycling in our clear-water study streams, but photorespiration and the Mehler reaction may increase during periods of highest light intensity during the day.

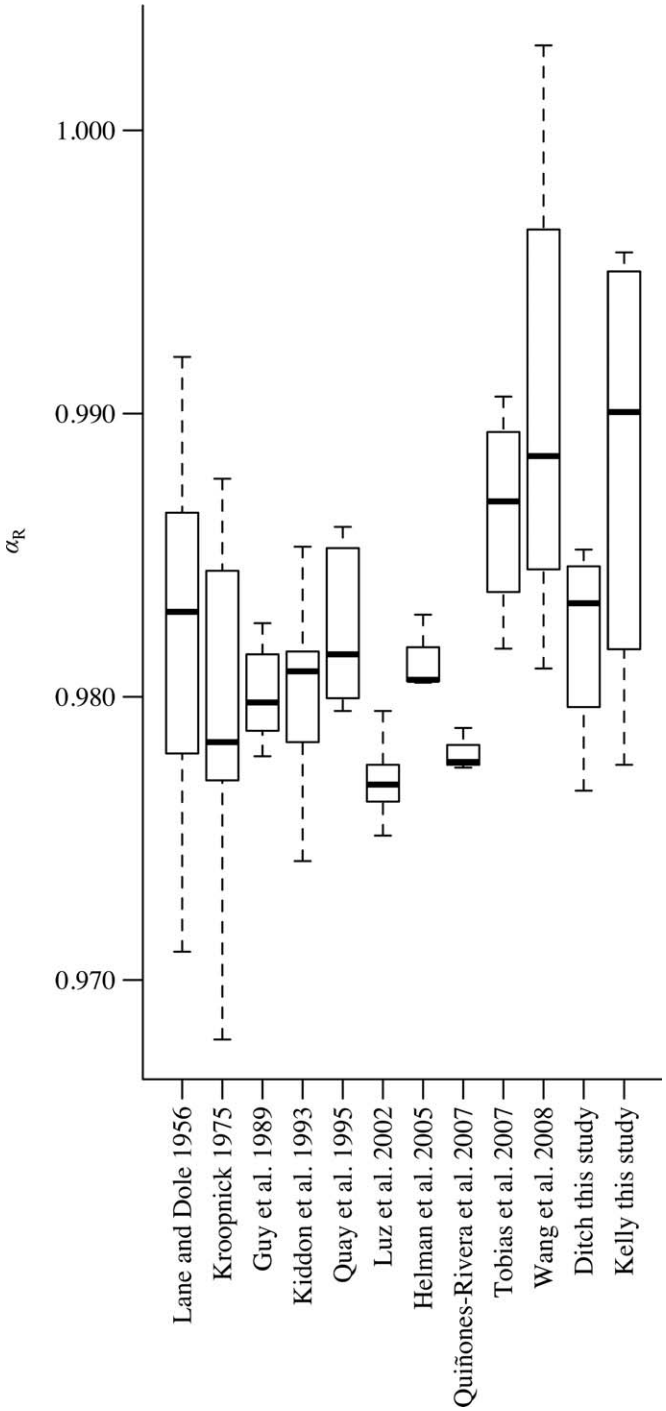

Fig. 3. Measurements of fractionation against $^{18}O_{O_2}$ during respiration (α_R) vary among studies. All published measurements were from static water or benthic incubations. Measurements from this study were made using dark flow-through benthic chambers. Whiskers represent the minimum and maximum values for α_R, boxes range from the first to third quartile, and the thick line within the box represents the median.

Temperature may increase ER during the daytime. Elevated temperatures can increase metabolic rates of organisms within their thermal tolerance range; Perkins et al. (2012) found a consistent relationship between temperature and ER in streams across a broad range of water temperatures. We used diel changes in water temperature to predict temperature-driven changes in ER, but the range of and maximum diel ER rates derived from O_2 temperature models were much lower than ranges and maximum diel ER rates estimated using $\delta^{18}O_{O_2}$ data (Fig. 2). Tobias et al. (2007) also compared diel estimates of ER from $\delta^{18}O_{O_2}$ with temperature-driven ER estimates. While the temperature and $\delta^{18}O_{O_2}$ model estimates of daytime ER were similar in the fall, $\delta^{18}O_{O_2}$ model-derived diel ER estimates were larger than temperature models could account for during the summer (Tobias et al. 2007).

ER and GPP can be coupled in freshwater ecosystems. Much of the respiration is from autotrophs themselves, especially on daily timescales (Hall and Beaulieu 2013; Solomon et al. 2013). GPP can also stimulate respiration by increasing concentrations of O_2 and/or organic compounds available for respiration (Weger et al. 1989; Epping and Jørgensen 1996). Algal exudation of DOC and nutrients may increase rates of daytime ER, which would not be included in temperature-driven metabolism models. Algae can release up to 75% of organic C fixed during photosynthesis into their surrounding environment, although the average release is likely closer to 15% (Baines and Pace 1991). This algal DOC tends to be highly biologically available for consumption by heterotrophic microbes and may support a large portion of secondary production and respiration (Cole et al. 1982; Moran and Zepp 1997; Farjalla et al. 2006). While gross rates of algal DOC release are difficult to measure directly because of rapid consumption by associated microbes, net algal DOC exudation rates can increase the total streamwater concentration of DOC during daytime (Kaplan and Bott 1982). Given the positive relationship between GPP and the magnitude of diel ER in our streams, we believe that GPP stimulated ER via higher rates of autotrophic respiration as well as DOC exudation and coupled heterotrophic respiration. Diel changes in production-driven ER likely account for much of the difference between the temperature-driven O_2 model and $\delta^{18}O_{O_2}$ model estimates of diel ER (Fig. 2).

Limitations of the diel $\delta^{18}O_{O_2}$ model—While we used diel $\delta^{18}O_{O_2}$ and O_2 data to estimate site-specific dielMET parameters for five sites in three streams and quantify the uncertainty associated with choice of α_R, our $\delta^{18}O_{O_2}$ dielMET estimates had large credible intervals in comparison to GPP_{base} and ER_{base} estimates (Table 2). By adding the dielMET parameter, we were able to assume diel measurements of dissolved O_2 were accurate and reflected the net diel changes in O_2 due to GPP, ER, and air–water gas exchange. The larger uncertainty in dielMET estimates could have been due to choices in model structure or limited power to estimate an additional unknown parameter with the data available. The uncertainty in dielMET estimates using our $\delta^{18}O_{O_2}$ data is also likely a result of fewer $\delta^{18}O_{O_2}$ measurements; we modeled $\delta^{18}O_{O_2}$ at 10 min time-steps, but we were only able to compare those modeled values with collected $\delta^{18}O_{O_2}$ data at 4 h time-steps. More frequent $\delta^{18}O_{O_2}$ data throughout each 24 h

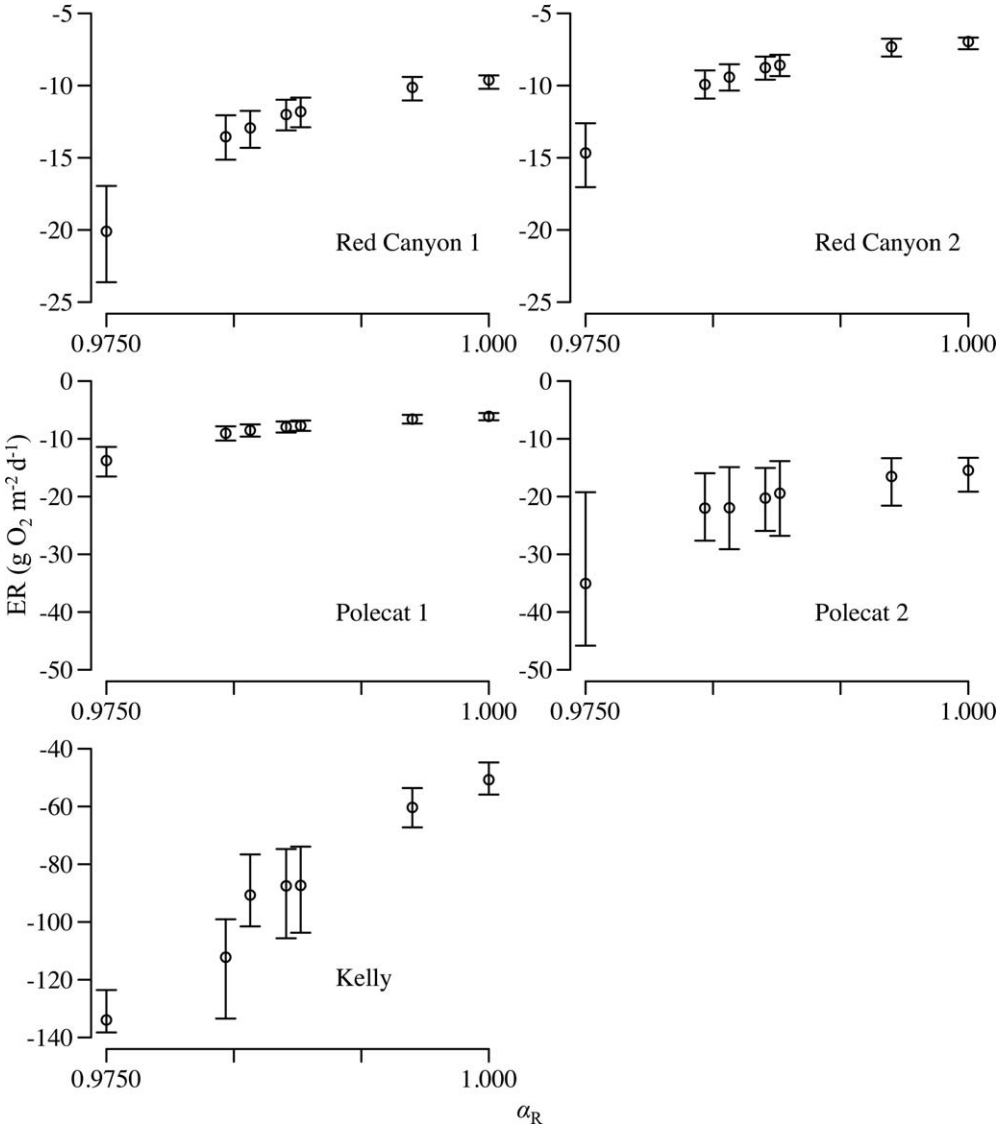

Fig. 4. Error in modeled diel ecosystem respiration (ER) increases as α_R (fractionation against $^{18}O_{O_2}$ during respiration) increases. Modeled estimates of ER are highly sensitive to the choice of α_R. Each point represents the mean modeled estimate of ER (ER = ER_{base} + [−dielMET]); Eq. 9b). Brackets represent the 2.5% and 97.5% Bayesian credible intervals.

period could help to better constrain the parameter estimates for dielMET and resulting diel ER and GPP calculations.

Direct measurements of the fractionation against $^{18}O_{O_2}$ during respiration are rare, especially measurements including benthic assemblages in flowing waters. Early α_R measurements focused on single species or assemblages in marine and lake water and were static chamber measurements made in the field or laboratory (Fig. 3). Tobias et al. (2007) were the first to include a benthic component, but they did not account for changes in α_R due to flowing water over the benthos. We included flowing water and benthic assemblages (on stream rocks) in our flow-through chamber measurements, but we still created an artificial environment using chambers. We used measured α_R in our $\delta^{18}O_{O_2}$ models, but we did not have flow-through chamber α_R estimates for each of the five specific sites on the dates and times of $\delta^{18}O_{O_2}$ data collection. The broad range of our α_R estimates (α_R = 0.9767–0.9957; Fig. 3) likely reflected patchiness of biological processes and α_R within the benthos, different processes driving net changes in $\delta^{18}O_{O_2}$ in dark chambers, and measurement error.

Diel estimates of ER using $\delta^{18}O_{O_2}$ metabolism models were sensitive to the value of α_R. Our modeling framework allowed us to show the uncertainty associated with one of the most sensitive parameters in the $\delta^{18}O_{O_2}$ model: α_R. However, we were unable to solve for α_R as another unknown parameter with the addition of the dielMET term. Fractionation likely varies over space and time, even within a single study reach during a single day. Wang et al. (2008) calculated α_R at a range of lake sites in different seasons; pelagic α_R estimates ranged from 0.981 to 1.001. To our knowledge, no one has measured diel changes in α_R. Considering the range of values for α_R in the literature as

well as the range of α_R estimates for a specific site across replications, sampling locations, times, and dates, the susceptibility of dielMET (and diel ER) to changes in α_R is troublesome. Estimates of dielMET in Kelly ranged from 12.1 to 95.5 g O_2 m^{-2} d^{-1}, depending on the choice of α_R (ranging from 0.975 to 1.000, respectively). While this was the largest range of dielMET estimates for the sites in our study, all site diel ER estimates depended heavily on choice of α_R (Fig. 4). We ultimately decided our chamber estimates were the best choice for α_R in our $\delta^{18}O_{O_2}$ models given the inclusion of benthos and flowing water, but estimates of diel ER would have been 1.5 times greater if we did not have chamber measurements and instead relied on the mean literature value for α_R ($\sim$0.982).

Metabolism estimates have been very sensitive to the choice of α_R in other models, even when the focus has been on daily estimates of GPP and ER and not diel changes in ER. For example, a model sensitivity analysis found that changing fractionation from 0.978 to 0.985 increased the ratio of GPP : ER by a factor of 3 (Quiñones-Rivera et al. 2009). Other $\delta^{18}O_{O_2}$ and O_2 model best fits in the literature required α_R values as high as 0.998 (Venkiteswaran et al. 2007). Assuming little or no fractionation against $\delta^{18}O_{O_2}$ during respiration allows for the use of $\delta^{18}O_{O_2}$ as an additional data set with which to constrain daily estimates of GPP and ER, but it prevents the use of diel $\delta^{18}O_{O_2}$ data to investigate the mechanisms driving diel rates of ER. Using α_R estimates from 0.995 to 1.000 to model diel ER for our study sites would have reduced dielMET estimates to one half or one tenth of dielMET using flow-chamber measurements of α_R. Despite the uncertainty associated with not knowing the "true" value of α_R appropriate for site- and time-specific estimates of ecosystem metabolism, Bayesian parameter estimation can be used to quantify this uncertainty while showing that daytime ER does indeed increase relative to nighttime rates, likely as a result of GPP driving increases in ER during the day.

The way forward—$\delta^{18}O_{O_2}$ may prove to be a powerful tool in enhancing our ability to estimate diel changes in ER and quantifying drivers of diel ER. Using diel changes in the natural abundance of $\delta^{18}O_{O_2}$, we modeled diel changes in ER for three streams in Wyoming, and we showed that ER, as measured by O_2, was greater in the daytime. Diel ER modeled using temperature-adjusted O_2 models did not account for the magnitude of diel ER swings estimated using $\delta^{18}O_{O_2}$, suggesting that GPP may drive diel changes in ER in these streams. Beyond the logistical and financial restrictions associated with diel sampling efforts and the cost to analyze $\delta^{18}O_{O_2}$ samples, three major challenges associated with $\delta^{18}O_{O_2}$ metabolism estimates remain: (1) identifying the role of O_2-cycling light reactions beyond mitochondrial respiration, (2) constraining α_R, and (3) acknowledging the uncertainty of parameter estimates to better inform within- and among-site comparisons of biological interest.

To estimate diel ER in the context of ecosystem C cycling, scientists must continue to examine how much of measured O_2 (whether dissolved O_2 or $\delta^{18}O_{O_2}$) cycling represents C cycling. This question of O_2 and C coupling could be a larger problem for $\delta^{18}O_{O_2}$ metabolism models, where estimates of ER depend on the choice of α_R and assume mitochondrial respiration is responsible for this fractionation. If estimates of diel ER made using O_2 measurements do not fully reflect C cycling, identifying other processes responsible for increased O_2 cycling during the day is of great interest. There is potential to quantify the relative contributions of different O_2 cycling processes using a combination of O_2 and C isotope tracers and estimates of process-specific isotope fractionation factors. Measurements at a larger scale than laboratory and field incubations are logistically more challenging but will likely yield more useful information for ecosystem-level metabolism calculations.

While higher frequency of $\delta^{18}O_{O_2}$ sampling will increase the precision of $\delta^{18}O_{O_2}$ model parameter estimates, the sensitivity of modeled ER to the choice of α_R will still be a major limitation of metabolism models using $\delta^{18}O_{O_2}$. Measurements of α_R should ideally match the spatial scale of O_2 measurements for metabolism estimates, but laboratory and field incubations can still provide valuable information about the range of realistic α_R values to use. Spatial and temporal heterogeneity in α_R is relatively unknown, especially for flowing waters and measurements made throughout diel cycles. Strategic combinations of laboratory and field measurements, coupled with modeling approaches that account for parameter uncertainty, could help us better understand α_R at the ecosystem level.

Bayesian parameter estimation provides a framework with which to compare model estimates with data to quantify the probability density distribution of metabolism parameters as a means of estimating parameter uncertainty. In this study, we could quantify diel rates of ER as well as the uncertainty in ER estimates associated with the range of α_R values in the literature. Further exploration of model structures and ways to quantify parameter uncertainty will greatly advance the confidence in our metabolism parameter estimates and how we identify the primary drivers associated with changes in GPP and ER.

To estimate the current and future role of freshwater ecosystems in regional and global C budgets, we require better estimates of freshwater ecosystem metabolism and better understanding of metabolism drivers. Various laboratory and field experiments and measurements, including this study, suggest that assuming constant rates of ER throughout 24 h cycles is unrealistic, which may limit our understanding of drivers of ecosystem metabolism and C cycling. What are the drivers of greater daytime vs. nighttime ER in aquatic ecosystems? To what extent do $\delta^{18}O_{O_2}$-derived diel estimates of ER reflect an increase in C oxidation? How can we use models to quantify the uncertainty in metabolism model parameter estimates? A better understanding of the relationships among light intensity, temperature, GPP, and C bioavailability in driving diel rates of ER will improve ecosystem metabolism models, with or without access to diel $\delta^{18}O_{O_2}$ data. Estimating rates of ER continues to be one of the biggest challenges associated with measuring C cycling in aquatic ecosystems, but improvements in data collection, metabolism models, and modeling approaches can enhance our

understanding of C processing and the role of freshwater ecosystems in regional and global C budgets.

Acknowledgments

T. Lehnertz, E. Anozko, R. Crosby, and S. Casebolt helped with laboratory and fieldwork for this project. H. Harlow and S. O'Ney provided logistical support for research in Grand Teton National Park, and L. Lautz and M. Mitchell provided support for research in Red Canyon. We thank N. Grimm for loaning us the flow-through chambers for fractionation measurements. B. Roberts provided valuable insights when starting this project. K. Ogle gave helpful feedback on earlier versions of our modeling framework. Comments from E. Pendall, D. Williams, M. Clementz, P. Colberg, C. Tobias, and an anonymous reviewer greatly improved this manuscript. Isotope samples were analyzed by the Wyoming Stable Isotope Facility ($\delta^{18}O_{H_2O}$) and the G. G. Hatch Stable Isotope Laboratory ($\delta^{18}O_{O_2}$).

Funding was provided by the University of Wyoming (Haub Creative Grant, Plummer Scholarship, Wyoming Science Teacher Education Program Summer Fellowship, Vern Bressler Fisheries Scholarship), a Sigma Xi Research Grant, the North American Benthological Society President's Endowment Award, and the National Science Foundation (Experimental Program to Stimulate Competitive Research 0447681 and Earth Sciences 0450317).

This manuscript is a contribution to the University of Wyoming–National Park Service Research Station.

References

Amado, A. M., V. F. Farjalla, F. de. A. Esteves, R. L. Bozelli, F. Roland, and A. Enrich-Prast. 2006. Complementary pathways of dissolved organic carbon removal pathways in clear-water Amazonian ecosystems: Photochemical degradation and bacterial uptake. FEMS Microbiol. Ecol. **56:** 8–17, doi:10.1111/j.1574-6941.2006.00028.x

Baines, S. B., and M. L. Pace. 1991. The production of dissolved organic matter by phytoplankton and its importance to bacteria: Patterns across marine and freshwater systems. Limnol. Oceanogr. **36:** 1078–1090, doi:10.4319/lo.1991.36.6.1078

Bender, M. K., and others. 1987. A comparison of four methods for determining planktonic community production. Limnol. Oceanogr. **32:** 1085–1098, doi:10.4319/lo.1987.32.5.1085

Brown, A. H. 1953. The effects of light on respiration using isotopically enriched oxygen. Am. J. Bot. **40:** 719–729, doi:10.2307/2439688

Carvalho, M. C., and B. D. Eyre. 2012. Measurement of planktonic CO_2 respiration in the light. Limnol. Oceangr.: Methods **10:** 167–178, doi:10.4319/lom.2012.10.167

Chomicki, K. M., and S. L. Schiff. 2008. Stable oxygen isotopic fractionation during photolytic O_2 consumption in stream waters. Sci. Total Environ. **404:** 236–244, doi:10.1016/j.scitotenv.2008.04.024

Cole, J. J., and N. F. Caraco. 1998. Atmospheric exchange of carbon dioxide in a low-wind oligotrophic lake measured by the addition of SF_6. Limnol. Oceanogr. **43:** 647–656, doi:10.4319/lo.1998.43.4.0647

———, G. E. Likens, and D. L. Strayer. 1982. Photosynthetically produced dissolved organic carbon: An important carbon source for planktonic bacteria. Limnol. Oceanogr, **27:** 1080–1090, doi:10.4319/lo.1982.27.6.1080

Craig, H. 1961. Standard for reporting concentration of deuterium and oxygen-18 in natural waters. Science **133:** 1833–1834, doi:10.1126/science.133.3467.1833

De Lange, H. D., D. Morris, and C. Williamson. 2003. Solar ultraviolet photodegradation of DOC may stimulate freshwater food webs. J. Plankton Res. **25:** 111–117, doi:10.1093/plankt/25.1.111

del Giorgio, P. A., and P. B. Williams. 2005. Respiration in aquatic ecosystems. Oxford Univ. Press.

Epping, E. H. G., and B. B. Jørgensen. 1996. Light-enhanced oxygen respiration in benthic phototrophic communities. Mar. Ecol. Prog. Ser. **139:** 193–203, doi:10.3354/meps139193

Farjalla, V. F., F. A. Esteves, R. L. Bozelli, F. Roland, and A. Enrich-Prast. 2006. Influence of hydrological pulse on bacterial growth and DOC uptake in a clear-water Amazonian lake. Microbial Ecol. **52:** 334–344, doi:10.1007/s00248-006-9021-4

Geyer, C. J., and L. T. Johnson. 2013. mcmc: Markov Chain Monte Carlo. R package version 0.9-2. Available from http://cran.r-project.org/package=mcmc

Guy, R. D., J. A. Berry, M. L. Fogel, and T. C. Hoering. 1989. Differential fractionation of oxygen isotopes by cyanide-resistant and cyanide-sensitive respiration in plants. Planta **177:** 483–491, doi:10.1007/BF00392616

Hall, R. O., and J. J. Beaulieu. 2013. Estimating autotrophic respiration in streams using daily metabolism data. Freshw. Sci. **32:** 507–516, doi:10.1899/12-147.1

Hanson, P. C., S. R. Carpenter, N. Kimura, C. Wu, S. P. Cornelius, and T. K. Kratz. 2008. Evaluation of metabolism models for free-water dissolved oxygen methods in lakes. Limnol. Oceanogr.: Methods **6:** 454–465, doi:10.4319/lom.2008.6.454

Helman, Y., E. Barkan, D. Eisenstadt, B. Luz, and A. Kaplan. 2005. Fractionation of the three stable oxygen isotopes by oxygen-producing and oxygen-consuming reactions in photosynthetic organisms. Plant Physiol. **138:** 2292–2298, doi:10.1104/pp.105.063768

Hilborn, R., and M. Mangel. 1997. The ecological detective: Confronting models with data. Princeton Univ. Press.

Holtgrieve, G. W., D. E. Schindler, T. A. Branch, and Z. T. A'mar. 2010. Simultaneous quantification of aquatic ecosystem metabolism and reaeration using a Bayesian statistical model of oxygen dynamics. Limnol. Oceanogr. **55:** 1047–1062, doi:10.4319/lo.2010.55.3.1047

Hotchkiss, E. R., and R. O. Hall. 2010. Linking calcification by exotic snails to stream inorganic carbon cycling. Oecologia **163:** 235–244, doi:10.1007/s00442-009-1536-1

Jackson, W. A., and R. J. Volk. 1970. Photorespiration. Annu. Rev. Plant Physiol. **21:** 385–432, doi:10.1146/annurev.pp.21.060170.002125

Jähne, B., G. Heinz, and W. Dietrich. 1987. Measurement of diffusion coefficients of sparingly soluble gases in water. J. Geophys. Res. **92:** 10767–10776, doi:10.1029/JC092iC10p10767

Kaplan, L. A., and T. L. Bott. 1982. Diel fluctuations of DOC generated by algae in a piedmont stream. Limnol. Oceanogr. **27:** 1091–1100, doi:10.4319/lo.1982.27.6.1091

Kiddon, J., M. L. Bender, and J. Orchardo. 1993. Isotopic fractionation of oxygen by respiring marine organisms. Glob. Biogeochem. Cy. **7:** 679–694, doi:10.1029/93GB01444

Kroopnick, P. M. 1975. Respiration, photosynthesis, and oxygen isotope fractionation in oceanic surface water. Limnol. Oceanogr. **20:** 988–992.

Lane, G. A., and M. Dole. 1956. Fractionation of oxygen isotopes during respiration. Science **123:** 574–576, doi:10.1126/science.123.3197.574

Luz, B., and E. Barkan. 2000. Assessment of oceanic productivity with the triple-isotope composition of dissolved oxygen. Science **288:** 2028–2031, doi:10.1126/science.288.5473.2028

———, ———, Y. Sagi, and Y. Z. Yacobi. 2002. Evaluation of community respiration mechanisms with oxygen isotopes: A case study in Lake Kinneret. Limnol. Oceanogr. **47:** 33–42, doi:10.4319/lo.2002.47.1.0033

Mehler, A. H., and A. H. Brown. 1952. Studies on reactions of illuminated chloroplasts. III. Simultaneous photoproduction and consumption of oxygen studied with oxygen isotopes. Arch. Biochem. Biophys. **38:** 365–370, doi:10.1016/0003-9861(52)90042-8

Moran, M. A., and R. G. Zepp. 1997. Role of photoreactions in the formation of biologically labile compounds from dissolved organic matter. Limnol. Oceanogr. **42:** 1307–1316, doi:10.4319/lo.1997.42.6.1307

Mulholland, P. J., and others. 2001. Inter-biome comparison of factors controlling stream metabolism. Freshw. Biol. **46:** 1503–1517, doi:10.1046/j.1365-2427.2001.00773.x

Odum, H. T. 1956. Primary production in flowing waters. Limnol. Oceanogr. **1:** 102–117, doi:10.4319/lo.1956.1.2.0102

Parker, S. R., and others. 2010. Diel behavior of stable isotopes of dissolved oxygen and dissolved inorganic carbon in rivers over a range of trophic conditions, and in a mesocosm experiment. Chem. Geol. **269:** 22–32, doi:10.1016/j.chemgeo.2009.06.016

Parkhill, K. L., and J. S. Gulliver. 1999. Modeling the effect of light on whole-stream respiration. Ecol. Model. **117:** 333–342, doi:10.1016/S0304-3800(99)00017-4

Perkins, D. M., and others. 2012. Consistent temperature dependence of respiration across ecosystems contrasting in thermal history. Global Change Biol. **18:** 1300–1311, doi:10.1111/j.1365-2486.2011.02597.x

Pringault, O., V. Tassas, and E. Rochelle-Newall. 2007. Consequences of respiration in the light on the determination of production in pelagic systems. Biogeosciences **4:** 105–114, doi:10.5194/bg-4-105-2007

Quay, P. D., D. O. Wilbur, J. E. Richey, A. H. Devol, R. Benner, R., and B. R. Forsberg. 1995. The $^{18}O:^{16}O$ of dissolved oxygen in rivers and lakes in the Amazon Basin: Determining the ratio of respiration to photosynthesis rates in freshwaters. Limnol. Oceanogr. **40:** 718–729, doi:10.4319/lo.1995.40.4.0718

Quiñones-Rivera, Z. J., B. Wissel, and D. Justić. 2009. Development of productivity models for the northern Gulf of Mexico based on oxygen concentrations and stable isotopes. Estuar. Coast. **32:** 436–446, doi:10.1007/s12237-009-9144-1

———, W. Wissel, D. Justić, and B. Fry. 2007. Partitioning oxygen sources and sinks in a stratified, eutrophic coastal ecosystem using stable oxygen isotopes. Mar. Ecol. Prog. Ser. **342:** 69–83, doi:10.3354/meps342069

R Development Core Team. 2012. R: A language and environment for statistical computing, reference index 2.15.2. R Foundation for Statistical Computing, Vienna, Austria. ISBN 3-900051-07-0, Available from http://www.R-project.org/.

Solomon, C. T., and others. 2013. Ecosystem respiration: Drivers of daily variability and background respiration in lakes around the globe. Limnol. Oceanogr. **58:** 849–866.

Tobias, C. R., J. K. Böhlke, and J. W. Harvey. 2007. The oxygen-18 isotope approach for measuring aquatic metabolism in high-productivity waters. Limnol. Oceanogr. **52:** 1439–1453, doi:10.4319/lo.2007.52.4.1439

Van de Bogert, M. C., S. R. Carpenter, J. J. Cole, and M. L. Pace. 2007. Assessing pelagic and benthic metabolism using free water measurements. Limnol. Oceanogr.: Methods **5:** 145–155, doi:10.4319/lom.2007.5.145

Venkiteswaran, J. J., L. I. Wassenaar, and S. L. Schiff. 2007. Dynamics of dissolved oxygen isotopic ratios: A transient model to quantify primary production, community respiration, and air–water exchange in aquatic ecosystems. Oecologia **153:** 385–398, doi:10.1007/s00442-007-0744-9

Wang, X., D. Depew, S. Schiff, and R. E. H. Smith. 2008. Photosynthesis, respiration, and stable isotopes of oxygen in a large oligotrophic lake (Lake Erie, USA–Canada). Can. J. Fish. Aquat. Sci. **65:** 2320–2331, doi:10.1139/F08-134

Wanninkhof, R. 1992. Relationship between wind speed and gas exchange over the ocean. J. Geophys. Res. **97:** 7373–7382, doi:10.1029/92JC00188

Weger, H. G., R. Herzig, P. G. Falkowski, and D. H. Turpin. 1989. Respiratory losses in the light in a marine diatom: Measurements by short-term mass spectrometry. Limnol. Oceanogr. **34:** 1153–1161, doi:10.4319/lo.1989.34.7.1153

Yard, M. E., G. E. Bennett, S. N. Mietz, L. G. Coggins, L. E. Stevens, S. Hueftle, and D. W. Blinn. 2005. Influence of topographic complexity on solar insolation estimates for the Colorado River, Grand Canyon, AZ. Ecol. Model. **185:** 157–172, doi:10.1016/j.ecolmodel.2004.07.027

Associate editor: Alexander D. Huryn

Received: 07 May 2013
Accepted: 20 November 2013
Amended: 02 February 2014